Journal of Thermal Analysis and Calorimetry
https://doi.org/10.1007/s10973-025-14656-0

Influence of octadecylammonium surfactant loading on vermiculite's structure, surfactant distribution and thermal properties

Hamoudi Belhoul[1,2] · Smail Terchi[1,2] · Naziha Ladjal[1,3] · Abdelhalim Zoukel[4] · Bahri Deghfel[1,5] · Issam Ziani[6] · Ahmad Azmin Mohamad[7]

Received: 24 August 2024 / Accepted: 5 August 2025

Abstract
Research was conducted to alter vermiculite by introducing linear octadecylammonium (ODA) cations into the interlayer spaces of the clay at different concentrations, ranging from 0.25 to 3 times the cation exchange capacity (CEC), to prepare organo-vermiculites (ODA-Vmt). This study aims to reveal a crucial mechanism of effective interaction between the surfactant and clay platelets, a detail overlooked in prior studies. The objective was to study the structural and property changes in vermiculite upon ODA cation intercalation. Characterization of the obtained ODA-Vmt was done using structural, morphology, elemental, thermal and bonding analysis. The elemental analysis confirmed successful cation exchange and surfactant intercalation, resulting in a hydrophobic surface. Morphologies revealed rougher textures in organo-vermiculite compared to raw vermiculite. The structural showed increased interlayer spacing with ODA loading, reaching saturation at 2CEC. Bonding analysis indicated strong interaction between ODA and clay, increasing hydrophobicity and thermal analysis showed decreased water-related mass loss and increased surfactant decomposition with higher ODA loading. The thermal analysis also shows that intercalation levels are higher at lower surfactant ($\leq$1CEC) concentrations, while surfactant adsorption increases at higher concentrations ($\geq$1CEC). This study provides valuable insights into the structure–property relationships of organo-vermiculite materials, highlighting their potential applications in pollutant remediation and advanced nanocomposite development.

Keywords Vermiculite · Clays · Intercalation · Adsorption · Cationic surfactants · Thermal analysis

Introduction

Organoclays (OCs) have received considerable attention recently due to their wide range of applications across various industries, such as fillers in clay-based polymer nanocomposites, rheological agents, starting materials in photophysical films, as well as organic pollutant adsorbents for water environments and soils [1, 2].

The OCs exhibited notably enhanced adsorption capability for organic contaminants compared to the pristine clay minerals [3]. Clay-polymer nanocomposites demonstrated heightened durability and heat resilience [4].

✉ Smail Terchi
smail.terchi@univ-msila.dz

✉ Ahmad Azmin Mohamad
aam@usm.my

[1] Laboratory of Materials and Renewable Energy, Faculty of Sciences, University of M'sila, University Pole, Road Bourdj Bou Arreiridj, 28000 M'sila, Algeria

[2] Department of Chemistry, Faculty of Science, University of M'sila, University Pole, Road Bourdj Bou Arreiridj, 28000 M'sila, Algeria

[3] Ecole Normale Supérieure de Boussaada, 28201 Boussaada, Algeria

[4] Laboratory Physico-Chemistry of Materials, Laghouat University, Laghouat, Algeria

[5] Department of Physics, Faculty of Sciences, University of M'sila, University Pole, Road Bourdj Bou Arreiridj, 28000 M'sila, Algeria

[6] Mineral Chemistry Laboratory, Faculty of Science and Technology, University of Mohamed El Bachir EL Ibrahimi- Bordj Bou Arreridj, Bordj Bou Arreridj, Algeria

[7] Energy Materials Research Group (EMRG), School of Materials and Mineral Resources Engineering, Universiti Sains Malaysia, 14300 Nibong Tebal, Pulau Pinang, Malaysia

Published online: 05 September 2025

OCs are typically produced by incorporating cationic surfactants into the interlayer space of clay minerals through the exchange of existing interlayer cations. The montmorillonite stands out as the most commonly employed clay mineral for crafting organoclays [5, 6]. Several studies have shown that the basal spacing of organo-montmorillonites expands as the quantity of loaded surfactant rises. The maximum basal spacing can be achieved when the loaded surfactant quantity exceeds one times the clay mineral's cation exchange capacity (CEC) [5, 7]. In such case, both the surfactant cation and molecule (ion-pair) can be inserted into the interlayer space, leading to notable alterations in the structure and characteristics of the resulting organomontmorillonite [8]. In montmorillonite-ammonium organoclays, surfactants exist in three environments: (1) intercalated into interlayer spaces and electrostatically bound, (2) physically adsorbed on the external surface, and (3) situated within the interlayer spaces [9].

The distribution of surfactants within organo-clays, particularly the specific percentages in distinct regions, is crucial for understanding the intercalation process, which has not been well explained in the literature. The preparation of organo-vermiculite remains limited as well. Vermiculite, a trioctahedral clay mineral with a 2:1 mica-type layered structure, contains octahedrally coordinated cations (Al(III), Mg(II), Fe(II)) and tetrahedrally coordinated cations (Si(IV), Al(III)). The substitution of central cations by lower valence cations creates a negative layer charge, balanced by interlayer hydrated cations like Mg(II), Ca(II), Na(I), and K(I) [10, 11]. The porous nature and low cost of vermiculite make it a potential replacement for conventional adsorbents [12]. Natural abundance, structure, chemical adaptability, recyclability, and high adsorption capability render it suitable for agricultural, industrial, and environmental applications. Current research focuses on the adsorption of dyes, heavy metals, antibiotic residues, and phenols using organo-vermiculite [3, 13–15]. Organo-vermiculites have shown potential for removing contaminants from water, but adsorption tests are beyond the scope of this study and will be explored in future work.

This study aims to synthesize organo-vermiculites characterized by both expanded basal spacing and hydrophobic surface properties. Furthermore, the percentages of surfactant distribution within the clay matrix are quantified. Vermiculite was used with higher layer charge density ($\hat{}$ 0.6 eq./formula unit) than Montmorillonite (< 0.6 eq./formula unit) and high CEC (128 mmol/100 g) to prepare organo-vermiculite. The organo-vermiculite (Org-Vmt) was created by purifying raw clay, sodifying, and intercalating with octadecylammonium (ODA) salts with different surfactant loadings. A comprehensive array of characterization methods was employed to scrutinize the structure, thermal stability, and hydrophobicity of the resulting organo-vermiculites.

Materials and methods

Materials

The experimental protocol included purifying raw clay, exchanging clay with sodium cations, and intercalating ODA onto sodic clay. Vermiculite adsorbent from CMMP (Paris, France) with a CEC of 128 mmol/100 g was used. The exchange process involved Ba^{2+} ions, and electrical conductivity curves were recorded to determine the equivalence point. Octadecylamine (ODA), $CH_3(CH_2)_{17}NH_2$, with a melting point of 55–57 °C (Sigma-Aldrich).

Purification of raw clay

The raw clay washed several times with distilled water and dried at 70 °C for 72 h. Retsch GmbH-Allee1-542,781 Haan, Germany, Type PM 100 planetary ball mill was used to grind the vermiculite before sieving. Every milling was done using a 10 g sample for 2h (30 min grinding with 10 min resting) in a 100 cm^3 Wolfram carbide mill chamber with 5 grinding balls (11 g), (2 cm diameter) and 320 rpm of rotation speed. The clay was sieved into granules of less than 90 µm. The obtained sample was denoted as raw Vmt and characterized by elemental analysis XRF, FTIR, XRD, MEB, EDX and TGA.

Sodification of vermiculite

The purified vermiculite sample (50 g) was immersed in a 0.128 M NaCl solution and heated at 70 °C with stirring for 8 h. The suspension was centrifuged (4000 rpm, 20 min) until no chloride ion was detected using a 0.1 M $AgNO_3$ test, confirmed by the absence of white precipitate. The precipitate was dried at 80°C for 24 h in a vacuum oven, milled, and sieved through 90 µm for further use. The treated sodium vermiculite, designated as Na-Vmt, was then characterized.

Organo-vermiculites preparation

Org-Vmts were prepared by cationic exchange between sodium vermiculite (Na-Vmt) and octadecylamine (ODA) in an aqueous solution. The process involved dispersing 7 g of Na-Vmt in 100 mL of hot distilled water (80 °C) with stirring for 1 h (mixture A). Separately, ODA was slowly dissolved in 250 mL of distilled water and hydrochloric acid (36%) at 80°C with stirring for 3 h (mixture B). The ODA amounts were adjusted to 0.25, 0.5, 0.75, 1.0, 2.0, and 3.0 CEC of Vmt. Mixtures A and B were combined and stirred at 80 °C for 5 h and left for 24 h. Organo-vermiculites were washed free of chloride anions with distilled water at

80 °C using $AgNO_3$ tests. The precipitates were centrifuged (4000 rpm, 20 min) and dried in an oven (80 °C, 24 h) to obtain modified vermiculites (Vmt-ODA). The intercalation process is shown in Fig. 1.

Characterizations

The obtained samples were characterized using various conventional techniques. Elemental analysis was performed using X-ray flurorecsence (XRF) (S2 PUMA, BRUKER). X-ray diffraction (XRD) data were analyzed using an X'Pert PRO MPD diffractometer. Fourier transform infrared spectroscopy (FTIR) measurements were conducted using a SHIMADZU IRSpirit QATR-S spectrometer. Scanning Electron Microscopy and Energy Dispersive X-ray Spectroscopy (SEM/EDS) images and data were acquired with a Quattro ESEM system. Thermogravimetric analysis (TGA) (SDT Q 600, TATGA) was performed under a nitrogen flow rate of 10 mL min^{-1}, with a heating rate of 10 °C min^{-1}, and a temperature range of 25–800 °C.

Results and discussion

Morphology and elements analysis

Firstly, the chemical composition (in mass percent) of raw Vmt, Vmt-Na, and Org-Vmts with different ODA loadings was determined using XRF. The analysis revealed that the interlayer cations are primarily potassium, calcium, and titanium ions, while the skeletal components (silicon, magnesium, aluminum, and iron) constitute 81.91% (Table 1). Comparison between raw clay and sodic vermiculite after sodification showed a decrease in Mg, Ca, and Co ratios, indicating replacement by Na^+ cations through cationic exchange [16]. Conversely, an increase in sodium was observed by EDS. Comparison between sodic vermiculite and Vmt-ODA showed the disappearance of sodium and a decrease in all components (SiO_2, MgO, Al_2O_3, Fe_2O_3, K_2O, TiO_2, CaO, Rb_2O, CoO, MnO), with a notable increase in loss on ignition as the CEC loadings increased. This decrease in mineral components in Vmt-ODA is attributed to

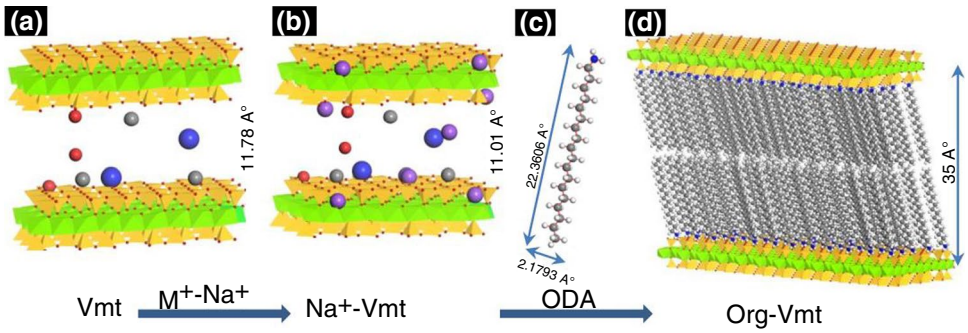

Fig. 1 **a** Vmt, **b** Na^+-Vmt with Na ions are designated by purple atoms, **c** structure of ODA surfactant, and **d** intercalation of ODA surfactant into interlayer spacing of Vmt, Structures, molecules and layers were constructed using the Materials Visualizer as implemented in the Materials Studio environment

Table 1 XRF results of raw Vmt, Na-Vmt and Vmt-ODA

Mass ratio/%	Raw Vmt	Na – Vmt	Vmt -ODA (0.25CEC)	Vmt -ODA (0.5CEC)	Vmt -ODA (0.75CEC)	Vmt -ODA (1CEC)	Vmt -ODA 2CEC	Vmt -ODA (3CEC)
SiO_2	36.14	36.84	35.20	32.25	30.02	28.71	24.57	21.27
MgO	26.64	26.59	22.96	20.21	18.84	17.96	14.48	11.91
Al_2O_3	9.64	9.68	9.48	8.62	7.97	7.57	6.24	5.27
Fe_2O_3	9.49	9.92	9.27	7.78	7.44	7.22	5.58	4.97
K_2O	6.00	6.09	5.04	4.32	3.63	3.11	2.40	2.82
TiO_2	1.14	1.20	1.09	0.93	0.90	0.74	0.71	0.65
Cl	0.06	0.87	0.89	1.45	1.49	1.86	1.77	4.81
CaO	0.28	0.26	0.16	0.06	0.06	0.04	0.03	0.04
Rb_2O	0.08	0.08	0.08	0.06	0.06	0.06	0.04	0.04
CoO	0.06	0.05	0.05	0.04	0.05	0.01	0.01	0.01
MnO	0.04	0.05	0.04	0.03	0.03	0.03	0.02	0.02
Loss Fire	10.00	8.00	15.58	24.01	29.41	32.5	44.10	47.98
∑	99.57	99.63	99.84	99.76	99.90	99.81	99.95	99.79

the modification process, where sodium cations are replaced by ODA salt cations**.**

EDS was employed to identify the chemical elements in the samples and quantify their relative abundance. Sodium content increased by 1.63% in the Na-Vmt sample compared to the raw Vmt sample (Fig. 2), indicating efficient incorporation of sodium into the vermiculite structure [17, 18]. Comparing Na-Vmt to Vmt-ODA, sodium was absent, and carbon content increased from 15.59% for 0.25CEC to 60.69% for 3CEC. Additionally, there was a decrease in mineral proportions (Fig. 3), indicating that sodium cations were replaced by ODA salt cations during modification. This successful surfactant insertion into the vermiculite structure is further confirmed by XRF results.

SEM analysis was utilized to examine the morphology and surface textures of particles before and after organo-modification. The raw-Vmt morphology (Fig. 2a) reveals a uniform layered silicate structure with a relatively smooth surface, along with fragments and flakes [19]. In Na-Vmt (Fig. 2b), sodium ions replace other cations (Mg^{2+}, Ca^{2+}) in the raw-Vmt interlayer, maintaining a lamellar structure as confirmed by XRF and EDS results (Fig. 3a–h). Na-Vmt exhibits a smooth surface covered by small fragments, typical of a clay layered structure. In contrast, ODA-Vmts (Fig. 2c–h) display a rougher, more uneven surface and a looser, more layered structure compared to Na-Vmt, indicating successful intercalation of surfactants into the Na-Vmt layer. Additionally, the darker color of the clay suggests increased thickness, highlighting variations in clay thickness after modification [20]. To better quantify the surface roughness and porosity of the modified and unmodified vermiculite samples, further analysis using surface profilometry or gas adsorption–desorption (BET) methods is recommended in future work.

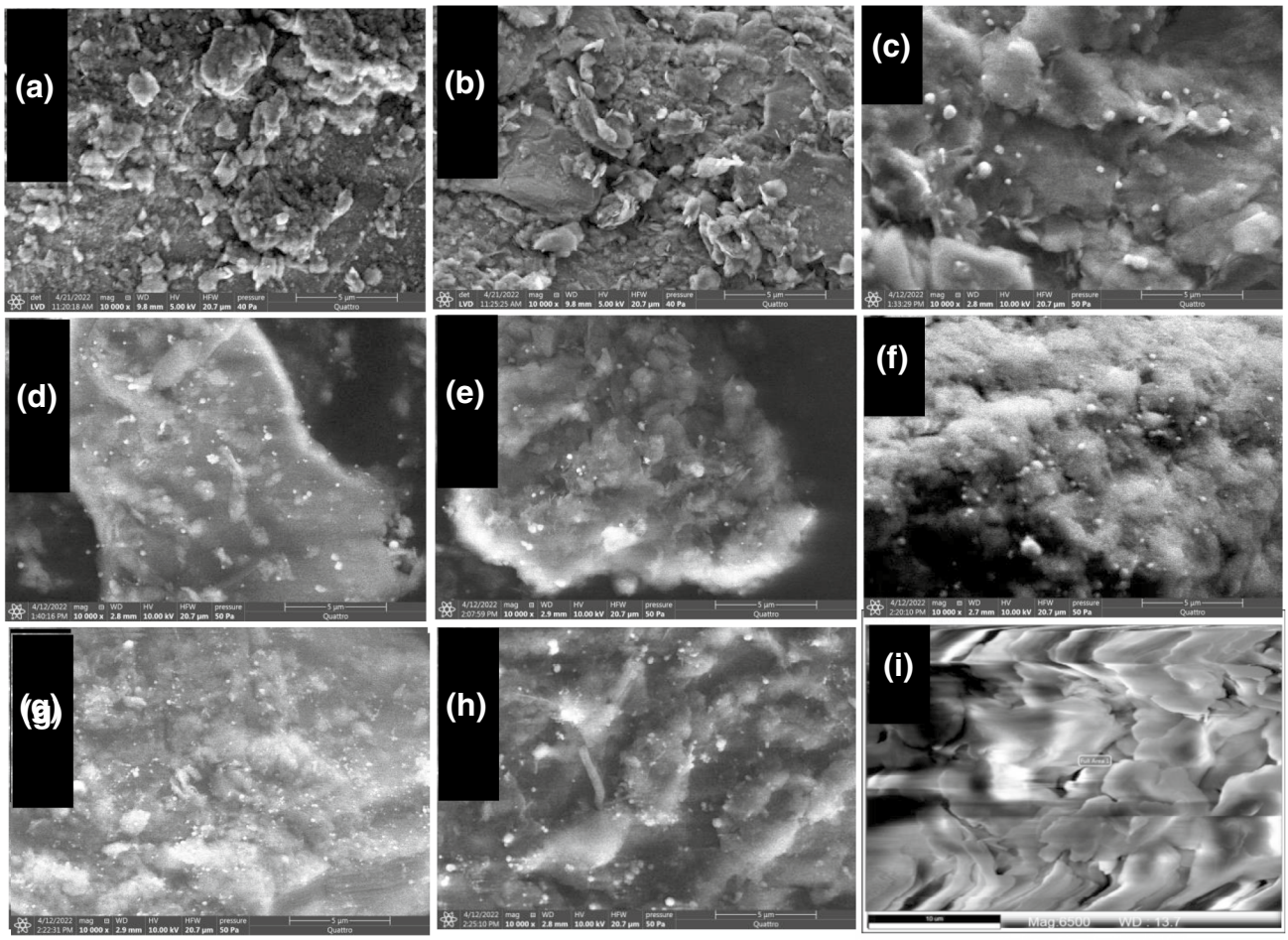

Fig. 2 Morphological observation for: **a** raw Vmt and **b** Na-Vmt; Vmt at various amounts of ODA surfactant: **c** 0.25CEC, **d** 0.5CEC, **e** 0.75CEC, **f** 1CEC, **g** 2CEC, **h** 3CEC, and **i** ODA

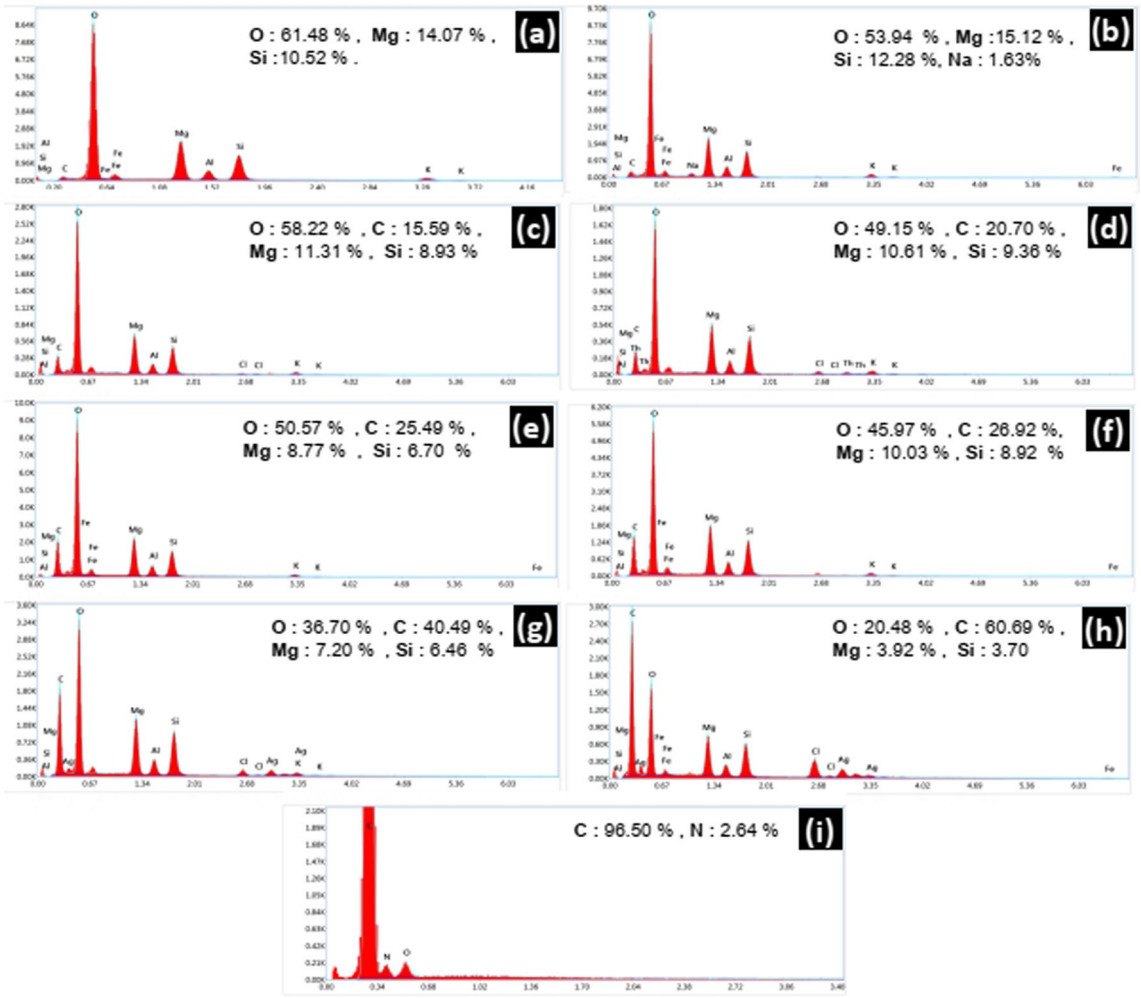

Fig. 3 EDS results of **a** raw Vmt, **b** Na-Vmt;Vmt at various amounts of ODA surfactant: **c** 0.25CEC, **d** 0.5CEC, **e** 0.75CEC, **f** 1CEC, **g** 2CEC, **h** 3CEC, and **i** ODA

Phase analysis

The X-ray spectra for ODA surfactant, raw Vmt, Na-Vmt, and Vmt-ODA are shown in Fig. 4. The basal spacing was determined using Bragg's equation. The peak for raw Vmt at $2\theta = 7.49°$ indicates a basal spacing of $d_{002} = 11.78$ Å. In contrast, Na-Vmt shows a lower basal spacing of $d_{002} = 11.01$ Å at 8.02°, indicating that Na^+ cations have replaced K^+, Ca^{2+}, and Mg^{2+} cations, confirming Na^+ intercalation in the Vmt interlayer [21].

Upon modification with ODA, significant changes are observed compared to unmodified Vmt. At lower ODA concentrations (≤ 1 CEC), there are no discernible reflections from the ODA salt in the Vmt-ODA samples, suggesting the absence of a physical mixture between the vermiculite and surfactant. The intensity of the Vmt reflection (11.01 Å) decreases until it disappears in Vmt-ODA (1 CEC), indicating effective modification through intercalation.

The XRD patterns of Vmt-ODA (2 CEC and 3 CEC) exhibit distinct reflections at 35 Å and 17.56–18.19 Å. The intercalation of ODA + cations into the interlayer space is confirmed by the shift of the Na-Vmt 002 peaks towards a lower 2θ following ion-exchange operations [15, 22]. The reaction can be represented as:

$$Na^+ - \text{Vermiculite} + \text{ODA} \rightarrow \text{ODA}^+ - \text{Vermiculite} + Na^+.$$

The basal spacing (d_{002}) of organo-vermiculite increases to a maximum of 35 Å for Vmt-ODA (2 CEC) and stabilizes for Vmt-ODA (3 CEC), indicating ODA saturation at 2 CEC concentration. Alkylammonium cations, known for intercalating in monolayer, bilayer, pseudo-trilayer, or paraffin structures within vermiculite sheets [23, 24], are regularly distributed in the interlayer space. This is evidenced by the high-intensity peak in the Org-Vmt XRD pattern at $2\theta = 2.52°$ ($d = 35$ Å). Subtracting the Vmt platelet thickness

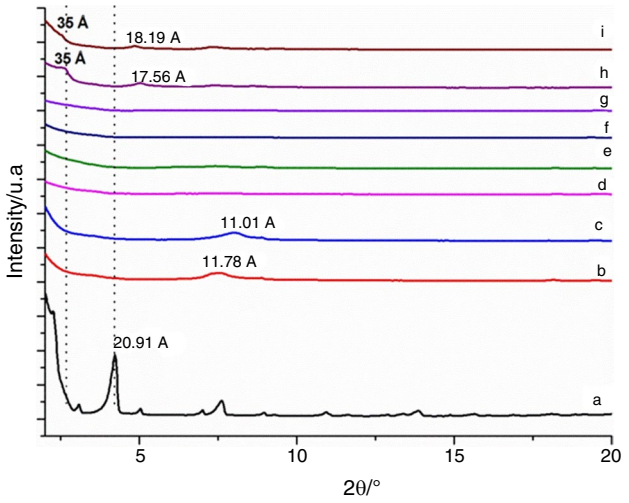

Fig. 4 XRD patterns of **a** ODA surfactant **b** raw Vmt, **c** Na-Vmt; Vmt at various amounts of ODA surfactant: **d** 0.25CEC, **e** 0.5CEC, **f** 0.75CEC, **g** 1CEC, **h** 2CEC and **i** 3CEC

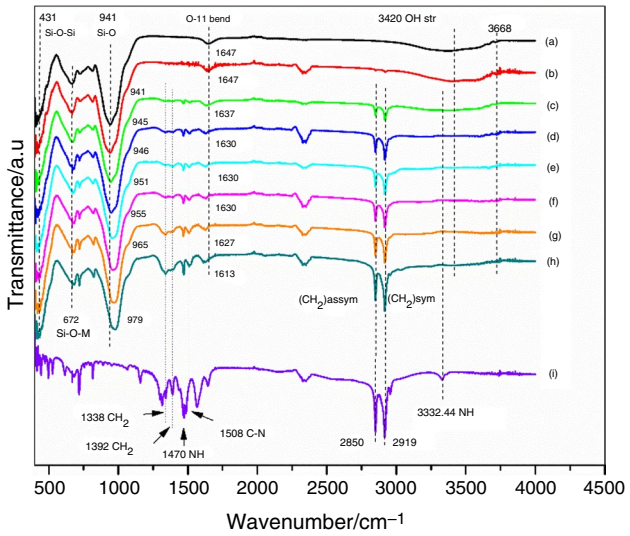

Fig. 5 FTIR spectra of **a** raw Vmt, **b** Na-Vmt; Vmt at various amounts of ODA surfactant: **c** 0.25CEC, **d** 0.5CEC, **e** 0.75CEC, **f** 1CEC, **g** 2CEC, **h** 3CEC, and **i** ODA

(~9.6 Å) from the d-spacing gives an interlayer distance of 25.36 Å, indicating that the ODA + cations formed a tilting paraffin-type bilayer configuration in the interlayer space (> 22 Å) [25–27].

Bonding analysis

Figure 5 shows the FTIR findings for vermiculite samples (raw-Vmt, Vmt-Na, and Vmt-ODA) within the vermiculite diagnostic ranges of 400–4000 cm^{-1}. The presence of hydroxyl groups in vermiculite is evidenced by the 3668 cm^{-1} band [15, [22]. Main bands appeared in raw Vmt, Na-Vmt and Vmt-ODA samples from FTIR spectra with their attributions are summarized in Table 2. The intercalation of Na^+ cations leads to an increase in the intensity of OH bands in Vmt-Na spectra, thereby creating a more hydrophilic surface [28]. This morphology corresponds to the distinctive bands of Na-Vmt that emerge in the presence of adsorbed water [19].

For Vmt-ODA, the interaction between Na-Vmt and surfactant cations resulted in the appearance of two peaks at 2850 cm^{-1} (symmetric) and 2919 cm^{-1} (antisymmetric) stretching vibrations of CH_2 in the alkyl chain [29]. These bands were confirmed by bending vibrations within the range of 1330–1423 cm^{-1} from CH_2 groups [30]. The removal of interlayer hydrated cations during ion exchange with alkylammonium groups decreased the intensity of OH bands at 3420 cm^{-1} and 1647 cm^{-1}, indicating a more hydrophobic surface compared to Na-Vmt [15, 29]. Increasing surfactant concentration strengthened the peaks for the alkyl chains. ODA exhibited a characteristic NH_2 peak at 3332 cm^{-1} (stretching), with the N–H bond vibrating at 1470 cm^{-1} [31], and a C–N bond stretching at 1507 cm^{-1} [32]. Higher surfactant concentrations shifted the Si–O band from 941 to 979 cm^{-1}, indicating bonding of ODA surfactant molecules with Si–O molecules through weak hydrogen bonds, confirming effective interaction between the surfactant and clay platelets.

Thermal analysis

TGA analysis investigates the thermodynamic stabilities of vermiculite compounds (raw Vmt, Na- Vmt, and Vmt-ODA).

Table 2 Main bands appeared in raw Vmt, Na-Vmt and Vmt-ODA samples from FTIR spectra with their attributions

ν/cm^{-1}	Attributions
431	Bending vibrations of Si–O–Si
672	Bending vibrations of Si–O-M (octahedral cation) (M = Al, Fe, Mg)
941	Si–O stretching vibration
1508	CN
1472	NH
1647	Bending vibrations of interlayer water O–H
1338–1392	CH bending vibrations
2850	Antisymmetric stretching vibrations of CH_2
2919	Symmetric stretching vibrations of CH_2
3332	NH stretching vibration
3420	Stretching vibrations of interlayer water O–H
3668	hydroxyl group

Figure 6 reveals temperature and mass loss associations. It shows three steps of modified vermiculite degradation:

Step 1, from 26 to 200 °C: involves the loss of water molecules either dissociated or adsorbed within particles interlayers [12, 33]. For raw Vmt, the mass loss is 5.76%, with DTG peaks at 75 °C and 180 °C, indicating the elimination of surface-adsorbed water and interlayer water associated with interlayer cations (Fig. 6a) [34]. Na-Vmt shows a slightly higher mass loss due to the more hydrated Na^+ cations, confirming the homoionization of vermiculite by Na^+ cations (Table 3, Fig. 6a–h). In this temperature range, the mass loss of Vmt-ODA decreases with increasing surfactant

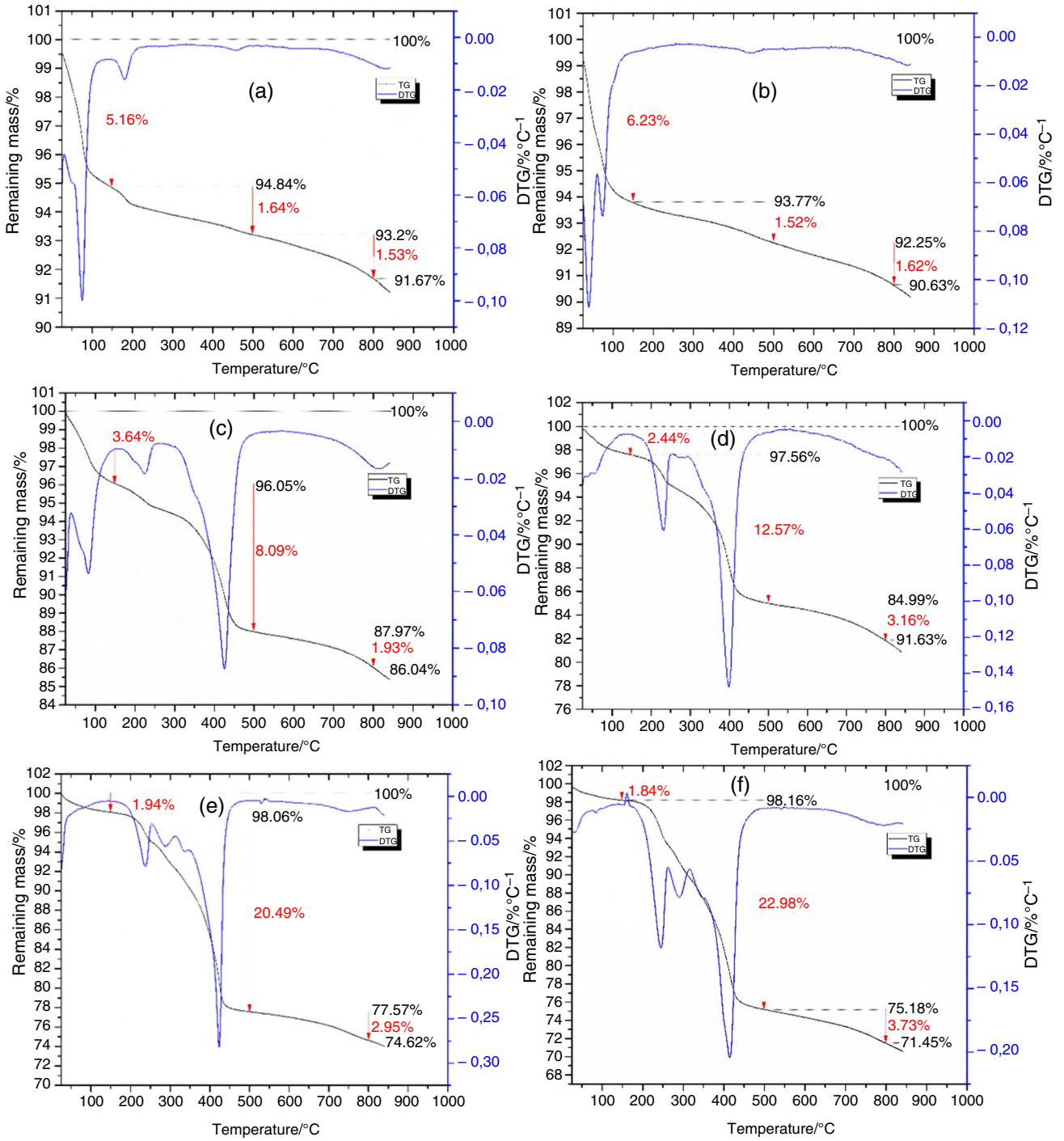

Fig. 6 TG-DTG results of **a** raw Vmt, **b** Na-Vmt; Vmt at various amounts of ODA surfactant: **c** 0.25CEC, **d** 0.5CEC, **e** 0.75CEC, **f** 1CEC, **g** 2CEC, **h** 3CEC, and **i** ODA

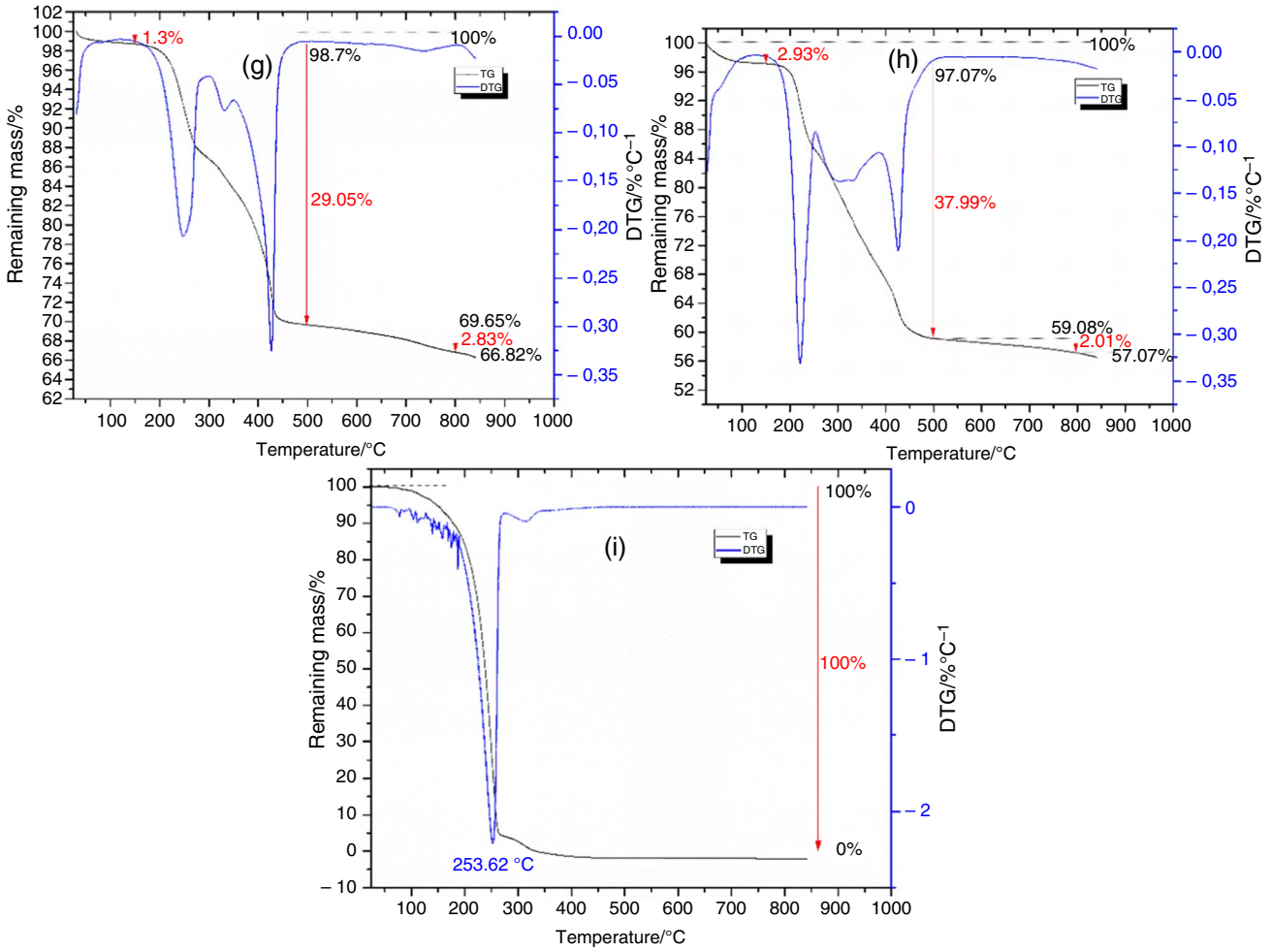

Fig. 6 (continued)

loading, suggesting enhanced hydrophobicity of the Na-Vmt surface following surfactant modification [35].

Step 2, from 200 to 500 °C: corresponds to the decomposition of the surfactant[5, 13]. The TG curve of the ODA sample shows a high mass loss (98%) at temperatures below 300 °C, with a maximum at 240 °C. Table 3 summarizes the mass loss values indicated by DTG peaks at various temperatures. During this step, Vmt-ODA decomposes in three phases: surface-adsorbed molecules decompose at about 220 °C, interlayer molecules at about 300 °C, and intercalated molecules at temperatures above 400 °C [1]. At surfactant loading levels of 1CEC or less, the mass loss related to intercalated surfactant is high (0.25 CEC: 85%, 0.5 CEC: 78%, 0.75 CEC: 74%, 1CEC: 69%), indicating intercalation as the primary interaction mechanism between the clay and surfactant. For ODA loading exceeding 1CEC, the mass loss related to intercalated surfactant decreases (2CEC: 50%, 3CEC: 25%) (Fig. 7a), while the mass loss associated with adsorbed and interlayer surfactants increases. Organo-vermiculite with high surfactant amounts (e.g., 3CEC) exhibits weak contact with the Vmt surface due to alkyl chain orientation and van der Waals force interaction (Fig. 7b) [36, 37]. The mass loss of Vmt-ODA within 200–500 °C indicates the quantity of surfactant in the samples, which can be compared with the amount added during preparation (Table 4). Below 1.0 CEC, the loaded surfactant amounts closely match those added, but they decrease beyond 1.0 CEC, with maximum loading occurring at concentrations above 2CEC.

Step 3, from 500 to 800 °C: involves the dihydroxylation of OH units in Vmt and the combustion of organic carbon and inorganic oxygen substances at temperatures above 700 °C for OVmt (Fig. 6a–h)[5, 38, 39].Table 3 summarizes the mass loss values indicated by DTG peaks at various temperatures. When ODA surfactant loading is ≤ 1CEC, the mass loss increases due to more carbon combusting with inorganic oxygen substances. Conversely, for ODA surfactant loading ≥ 1CEC, the mass loss

Table 3 TG/DTG results of raw Vmt, Na-Vmt, Vmt-ODA (0.25CEC, 0.5CEC, 0.75CEC, 1CEC, 2CEC, 3CEC), and ODA

	Step 1 Ambiant-200 °C		Step 2 200–500°C			Step 3 500-800°C	
	WL%	T max/°C	WL%		T max/°C	WL%	T max/°C
Raw Vmt	5.16	75	1.64	1.02	182	1.53	698
				0.62	456		
Na-Vmt	6.23	39	1.52		449	1.62	690
		74					
Vmt-ODA (0.25 CEC)	3.94	83	8.09	1.37	225	1.93	712
				6.72	425		
Vmt-ODA (0.5 CEC)	2.44	63	12.57	2.69	232	3.16	718
				9.88	399		
Vmt-ODA (0.75 CEC)	1.94	80	20.49	3.06	237	2.95	730
				2.78	289		
				1.84	338		
				12.81	423		
Vmt-ODA (1 CEC)	1.84	84	22.98	4.84	245	3.73	730
				3.64	291		
				14.5	415		
Vmt-ODA (2 CEC)	1.3	79	29.05	11.93	249	2.9	732
				3.2	332		
				13.92	426		
Vmt-ODA (3 CEC)	2.93	53	37.99	12.93	222	2.01	735
				16.4	315		
				9.62	426		
ODA	Ambiante-300 °C			–			–
	WL% 98	T max/°C 230					
	98	230					

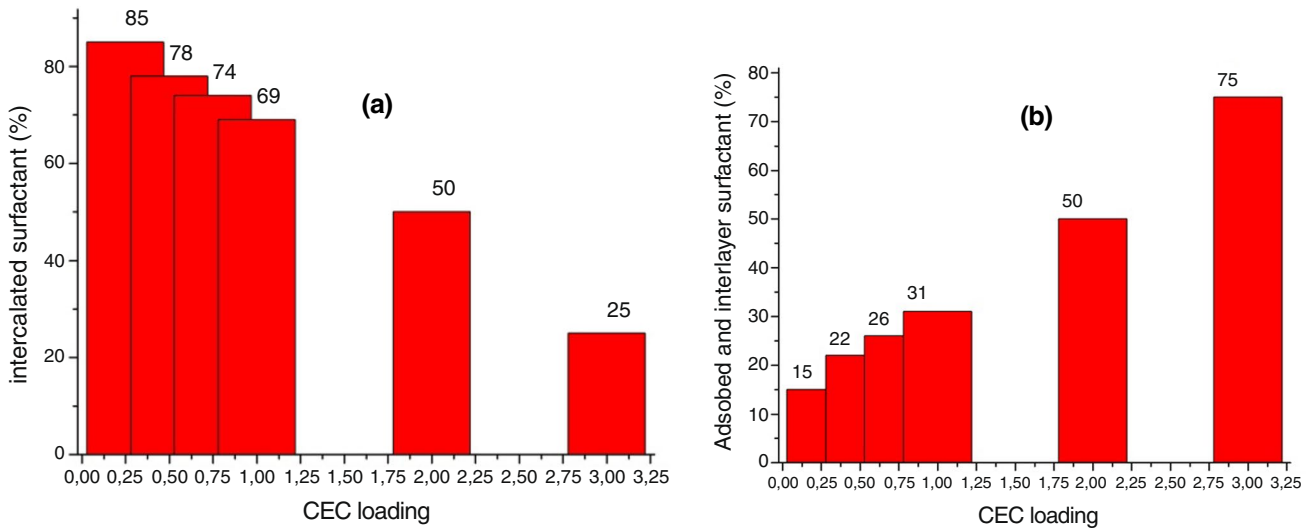

Fig. 7 **a** Variation of the percentage of intercalated surfactant and **b** the percentage of adsorbed and interlayer surfactant on vermiculite as a function of CEC loading

Table 4 comparison between the quantities of surfactant added to and loaded onto vermiculite

Samples	Amount of added surfactant (CEC)	Amount of loaded surfactant (CEC)
Vmt-ODA(0.25CEC)	0.25	0.25
Vmt-ODA(0.5CEC)	0.5	0.44
Vmt-ODA(0.75CEC)	0.75	0.70
Vmt-ODA(1CEC)	1	0.81
Vmt-ODA(2CEC)	2	1.1
Vmt-ODA(3CEC)	3	1.2

decreases because the surfactant adsorbed on the external clay decomposes at lower temperatures.

Conclusions

This study demonstrates the successful synthesis of organo-vermiculite (Vmt-ODA) with varying surfactant loadings, aimed at enhancing its basal spacing and hydrophobicity for applications in pollutant adsorption and polymer/organoclay nanocomposites. Main findings are:

i. Purification, Modification, and Chemical Composition: Raw vermiculite was purified, sodified, and intercalated with octadecylammonium (ODA) salts. XRF and EDS analyses confirmed successful cation exchange and surfactant intercalation, resulting in a hydrophobic surface.
ii. Interlayer Spacing, Chemical Bonding, and Surface Morphology: XRD analysis revealed expanded interlayer spacing with increasing ODA loading, indicating successful intercalation and formation of a paraffin-type bilayer configuration. FTIR spectroscopy showed the emergence of characteristic peaks corresponding to alkyl chain vibrations and a decrease in hydroxyl group intensities, confirming enhanced hydrophobicity. SEM analysis revealed rougher textures in organo-vermiculite samples compared to raw vermiculite, further confirming surfactant intercalation.
iii. Thermal Stability: TGA analysis showed a decrease in mass loss associated with water removal and an increase in surfactant decomposition as ODA loading increased. The thermal analysis indicates also higher degrees of intercalation at lower surfactant concentrations and enhanced surfactant adsorption at higher concentrations.

Acknowledgements S. Terchi, A. Zoukel and B. Deghfel thank the Algerian Ministry of Higher Education and Scientific Research represented by the Thematic Research Agency in Health and Life Sciences (TRAHLS) for financial support under the National Research Programs (NRP).

Author contributions HB was contributed to elaboration, characterization, methodology, data curation, investigation, writing review and editing. ST was contributed to methodology, data curation, writing review and editing. NL was contributed to characterization and data curation. AZ was contributed to characterization. BD was contributed to writing review and editing. IZ was contributed to characterization. AAM was contributed to writing review and editing.

References

1. Guégan R. Organoclay applications and limits in the environment. C R Chim. 2019;22:132–41.
2. Baldissera AF, Ferreira CA. Clay-based conducting polymer nanocomposites. 2017; p 143–63. https://doi.org/10.1007/978-3-319-46458-9_5
3. Batista LFA, de Mira PS, De Presbiteris RJB, Grassi MT, Salata RC, Melo VF, et al. Vermiculite modified with alkylammonium salts: characterization and sorption of ibuprofen and paracetamol. Chem Pap. 2021;75:4199–216. https://doi.org/10.1007/s11696-021-01643-6.
4. Terchi S, Hamrit S, Ladjal N, Bachari K, Ben Rhaiem H. Synthesize of exfoliated poly-methylmethacrylate/organomontmorillonite nanocomposites by in situ polymerization: structural study, thermal properties and application for removal of azo dye pollutant. J Therm Anal Calorim. 2024. https://doi.org/10.1007/s10973-023-12810-0.
5. Zidelkheir B, Abdelgoad M. Effect of surfactant agent upon the structure of montmorillonite X-ray diffraction and thermal analysis. J Therm Anal Calorim. 2008;94:181–7.
6. Sahnoun S, Boutahala M, Tiar C, Kahoul A. Adsorption of tartrazine from an aqueous solution by octadecyltrimethylammonium bromide-modified bentonite: kinetics and isotherm modeling. Comptes Rendus Chim. 2018;21:391–8.
7. Zhu J, Shen W, Ma Y, Ma L, Zhou Q, Yuan P, et al. The influence of alkyl chain length on surfactant distribution within organomontmorillonites and their thermal stability. J Therm Anal Calorim. 2012;109:301–9.
8. Xi Y, Zhou Q, Frost RL, He H. Thermal stability of octadecyltrimethylammonium bromide modified montmorillonite organoclay. J Colloid Interface Sci. 2007;311:347–53.
9. Xi Y, Frost RL, He H, Kloprogge T, Bostrom T. Modification of Wyoming montmorillonite surfaces using a cationic surfactant. Langmuir. 2005;21:8675–80.
10. Wang A, Wang W. Vermiculite nanomaterials: structure, properties, and potential applications. In: Nanomaterials from clay minerals: a new approach to green functional materials. Amsterdam: Elsevier; 2019. p. 415–844.
11. Hundáková M, Tokarský J, Valášková M, Slobodian P, Pazdziora E, Kimmer D. Structure and antibacterial properties of polyethylene/organo-vermiculite composites. Solid State Sci. 2015;48:197–204.
12. Zang W, Gao M, Shen T, Ding F, Wang J. Facile modification of homoionic-vermiculites by a gemini surfactant: comparative adsorption exemplified by methyl orange. Colloids Surf A Physicochem Eng Asp. 2017;533:99–108. https://doi.org/10.1016/j.colsurfa.2017.08.005.
13. Ji Y, Zhong H, Chen P, Xu X, Wang Y, Wang H, et al. Single and simultaneous adsorption of methyl orange and p-chlorophenol on

organo-vermiculites modified by an asymmetric gemini surfactant. Coll Surf A: Physicochem Eng Aspects. 2019;580:123740.
14. Wang J, Gao M, Shen T, Yu M, Xiang Y, Liu J. Insights into the efficient adsorption of rhodamine B on tunable organo-vermiculites. J Hazard Mater. 2019;366:501–11.
15. Tuchowska M, Wołowiec M, Solińska A, Kościelniak A, Bajda T. Organo-modified vermiculite: preparation, characterization, and sorption of arsenic compounds. Minerals. 2019. https://doi.org/10.3390/min9080483.
16. Feng J, Liu M, Mo W, Su X. Heating temperature effect on the hygroscopicity of expanded vermiculite. Ceram Int. 2021;47:25373–80.
17. Moraes DS, Rodrigues EMS, Lamarão CN, Marques GT, Rente AFS. New sodium activated vermiculite process. Testing on Cu^{2+} removal from tailing dam waters. J Hazard Mater. 2019;366:34–8. https://doi.org/10.1016/j.jhazmat.2018.11.086.
18. Długosz O, Banach M. Kinetic, isotherm and thermodynamic investigations of the adsorption of Ag+ and Cu2+ on vermiculite. J Mol Liq. 2018;258:295–309. https://doi.org/10.1016/j.molliq.2018.03.041.
19. Mao S, Shen T, Han T, Ding F, Zhao Q, Gao M. Adsorption and co-adsorption of chlorophenols and Cr(VI) by functional organo-vermiculite: experiment and theoretical calculation. Sep Purif Technol. 2021;277:119638. https://doi.org/10.1016/j.seppur.2021.119638.
20. Ding F, Gao M, Shen T, Zeng H, Xiang Y. Comparative study of organo-vermiculite, organo-montmorillonite and organo-silica nanosheets functionalized by an ether-spacer-containing Gemini surfactant: Congo red adsorption and wettability. Chem Eng J. 2018;349:388–96.
21. Melouki A, Terchi S, Ouali D, Bounab A. Preparation of new copolymer (polystyrene / TMSPM grafted on DDA - fractionated algerian montmorillonite) hybrid organoclay by radical copolymerization: structural study, thermal stability and hydrophobicity area. J Therm Anal Calorim. 2021. https://doi.org/10.1007/s10973-021-10935-8.
22. Lv W, Shen T, Ding F, Mao S, Ma Z, Xie J, et al. A novel NH2-rich polymer/graphene oxide/organo-vermiculite adsorbent for the efficient removal of azo dyes. J Mol Liq. 2021. https://doi.org/10.1016/j.molliq.2021.117308.
23. Lagaly G. <Solidsi22–43.Pdf>. 1986; 22:43–51.
24. Lagaly G. Characterization of clays by organic compounds. Clay Miner. 1981;16:1–21.
25. Wang L, Wang X, Chen Z, Ma P. Effect of doubly organo-modified vermiculite on the properties of vermiculite/polystyrene nanocomposites. Appl Clay Sci. 2013;75–76:74–81.
26. Xiong B, Mao S, Ding F, Shen T, Wang J, Jin X, et al. Comparative adsorption of polycylic aromatic compounds on organo-vermiculites modified by imidazolium- and pyridinium-based gemini surfactants. Coll Surf A Physicochem Eng Aspect. 2021;631:127701.
27. Jaynes WF, Boyd SA. Clay mineral type and organic compound sorption by hexadecyltrimethlyammonium-exchanged clays. Soil Sci Soc Am J. 1991;55:43–8.
28. Melouki A, Terchi S, Ouali D. Grafting of 3 mercaptopropyl triethoxysilane onto dodecylamuonium intercaled Algerian montmorillonite; characterizations and application for synthesis of polystyrene / organoclay hybrid material by radical polymerization. J New Technol Mater. 2021;11:10–8.
29. Ladjal N, Zidelkheir B, Terchi S. Influence of octadecylammonium, N, N-dimethylhexadecylammonium, and 1-hexadecyltrimethylammonium chloride upon the fractionated montmorillonite: thermal stability. J Therm Anal Calorim. 2018;134:881–8. https://doi.org/10.1007/s10973-018-7237-4.
30. Benítez JJ, San-Miguel MA, Domínguez-Meister S, Heredia-Guerrero JA, Salmeron M. Structure and chemical state of octadecylamine self-assembled monolayers on mica. J Phys Chem C. 2011;115:19716–23.
31. Sun M, Guo H, Zheng J, Wang Y, Liu X, Li Q, et al. Hydrophobic octadecylamine-polyphenol film coated slow released urea via one-step spraying co-deposition. Polym Test. 2020;91:106831. https://doi.org/10.1016/j.polymertesting.2020.106831.
32. Cao X, Wu S, Yang L, Cui J, Wang C, Li A. Novel composite phase change materials based on hollow carbon nanospheres supporting fatty amines with high light-to-thermal transition efficiency. Solar Energy Mater Solar Cells. 2021;225:111305.
33. Yu M, Gao M, Shen T, Wang J. Organo-vermiculites modified by low-dosage Gemini surfactants with different spacers for adsorption toward p-nitrophenol. Colloids Surf A Physicochem Eng Asp. 2018;553:601–11.
34. Dultz S, An JH, Riebe B. Organic cation exchanged montmorillonite and vermiculite as adsorbents for Cr(VI): effect of layer charge on adsorption properties. Appl Clay Sci. 2012;67–68:125–33. https://doi.org/10.1016/j.clay.2012.05.004.
35. Holešová S, Štembírek J, Bartošová L, Pražanová G, Valášková M, Samlíková M, et al. Antibacterial efficiency of vermiculite/chlorhexidine nanocomposites and results of the in vivo test of harmlessness of vermiculite. Mater Sci Eng C Mater Biol. 2014;42:466–73. https://doi.org/10.1016/j.msec.2014.05.054.
36. Liu S, Wu P, Yu L, Li L, Gong B, Zhu N, et al. Preparation and characterization of organo-vermiculite based on phosphatidylcholine and adsorption of two typical antibiotics. Appl Clay Sci. 2017;137:160–7.
37. Keawkumay C, Jarukumjorn K, Wittayakun J, Suppakarn N. Influences of surfactant content and type on physical properties of natural rubber/organoclay nanocomposites. J Polym Res. 2012. https://doi.org/10.1007/s10965-012-9917-2.
38. Önal M, Sarıkaya Y. Thermal analysis of some organoclays. J Therm Anal Calorim. 2008;91:261–5.
39. Marcos C, Lahchich A, Álvarez-Lloret P. Hydrothermally treated vermiculites: ability to support products for CO_2 adsorption and geological implications. Appl Clay Sci. 2023;232:106791.